The mechanics of eddy transport from one hemisphere to the other

Nathan Paldor and Andrey Sigalov

Institute of Earth Sciences
The Hebrew University of Jerusalem
Jerusalem, 91904 Israel

And

Doron Nof

School of Oceanography
Florida State University
Tallahassee, FL 32306

09 July, 2002; *QJRMS*, Submitted.

Abstract

The trajectory of a dense eddy that propagates along the bottom of a meridional channel of parabolic cross-section from the Southern to the Northern Hemisphere is described by a two-degrees-of-freedom, Hamiltonian, system. Two simplified types of motion exist in which to first order the meridinal acceleration vanishes. In mid-latitudes the motion is geostrophic, poleward (equatorward) directed along the channel's west (east) flank. On the other hand, right on the equator the motion is describable by linear oscillations along the potential-well generated by the channel's parabolic bottom cross-section. The propagation speed along the equator is much larger than that in mid-latitudes, which enhances the eddy's dissipation via its mixing with overlying ocean water. For motions that occur slightly off the equator the eastward segment is stable while the westward segment is unstable so an expulsion from the equatorial regime takes place during the latter. A dense eddy that arrives near the equator along the channel's west flank has to cross the channel to its east flank where it can either oscillate back (westward) to the other side of the channel or move poleward from the equator along the channel's east flank. The eddy's dissipation during the equatorial part of its trajectory is very large and the probability of the dissipated eddy leaving the equator to either of the two Hemispheres is identical.

The non-integrability of the system manifests itself in the sensitive combination of the equatorial, and the mid-latitude, regimes that renders the dynamics of the transport of AABW eddies to the Northern Hemisphere – chaotic. This description explains both the sharp decrease in the amount of AABW water mass in the immediate vicinity of the equator in the Western Atlantic Ocean and the "splitter" effect of the equator encountered in numerical simulations.

1. Introduction

The precise way in which the dense Antarctic Bottom Water (AABW) makes its way from Antarctica, across equator and into the Northern Hemisphere along the ocean's bottom has intrigued oceanographers for over 4 decades. The conjecture regarding the existence of deep (below 2000m) equatorward flow along the ocean's floor was first raised by Stommel (1958) based only on a simple thermally driven convective model and general consideration regarding the distribution of oxygen and temperature in the deep ocean. The dynamics of this slow, but high transport, flow (about 0.03 cm/s and 50 Sv according to Stommel) was the subject of numerous theoretical, computational and observational works that have all tried to better quantify and ascertain the existence of this flow. Even though there have not been any direction observations of eddies on the ocean bottom, it makes sense to assume that some of the transport is discontinuous and that, just like the upper ocean, some of the transport probably occurs via eddies (see e.g. Borisov and Nof, 1998). Our goal in this work is to analyze the dynamics associated with the dense eddies' transport from the high latitudes of the Southern Hemisphere into the Northern Hemisphere from a mechanical viewpoint and explain several features of this transport that are directly observed or indirectly inferred based upon various indications.

Observational and theoretical advances that were made during the four decades that elapsed from Stommel's original work are summarized in Nof and Borisov (1998, hereafter, NB) to which we refer the reader for a more complete review of the subject. The present study complements the theoretical works of NB and Borisov and Nof (1998) by casting both the equatorward motion from high latitudes (of the Southern Hemisphere) and the equator crossing problems into Hamiltonian systems. As was shown in NB the particle, Lagrangian, formulation of the problem equator-crossing by deep ocean eddies yields similar results to those obtained from simulations of a continuous current by an Ocean General Circulation Model (OGCM). This

result lends credence to the notion, adopted in the present study, that a particle analysis is relevant to the AABW transport into the Northern Hemisphere. In addition, the motion of eddies is best described by following their center-of-mass so if AABW is transported by eddies, a particle model (where the azimuthal velocity de-couples from the translation) is the most appropriate approach.

In what follows we briefly review only those elements of the AABW transport scenario that are relevant to the application of analytical mechanics.

(a) Equatorward flow from Antarctica

A precise, widely acceptable definition of the AABW characteristics does not exist in the literature but the term is broadly attributed to potential temperature of less than 1.9°C at depths exceeding 4000 meters (Whitehead and Worthington, 1982). As is clearly evident from the meridional sections shown in the Whitehead and Worthington work (see their Fig. 1), AABW occupy the depths exceeding 4000 m in the Western North Atlantic as far North as 40°N latitude. (Strictly speaking, this water is actually "modified Antarctic water" as the water has been modified by mixing during its long Northward flow from the South Atlantic but AABW has been used for very long time and, in addition, the Antarctic origin of the cold water justify its continual usage.) The potential temperature of the overlying North Atlantic Deep Water is more than 2°C and they occupy the depth between 1500 m and 4000 m in the Western North Atlantic so vertical mixing entails a downward flux of heat.

The inertial current model of Stommel and Arons (1960a,b) views the AABW flow as a current flowing equatorward as a western boundary current along the flank of a channel that extends from the High Latitudes of the Southern Hemisphere, to the equator. This Stommel and Arons theory deals only with the flow of (a column of) water from its source near the pole to the vicinity of the equator but ignores the equator crossing to the other Hemisphere.

A straightforward consideration of the angular momentum conservation indicates that a parcel of AABW originating at, say, 55°S latitude with a zero initial zonal velocity has increased its angular momentum, upon reaching the equator, by an amount equivalent to an increase of its zonal velocity to 200 m/s! How does this change of angular momentum take place without a corresponding increase in its kinetic energy? A careful account of the changes in angular momentum that a deep-water eddy undergoes on its way from Antarctica to the equator is the first issue addressed by the present study.

(b) *Equator crossing*

The process of equator-crossing by an AABW water parcel is not addressed by the Stommel and Arons theory but subsequent theoretical work on the subject stressed the possible role of either dissipation or relative vorticity changes along the western boundary. The reader is referred to NB for a thorough review on this important issue. Despite the basic differences between the dynamics of isolated eddies, modeled as point masses, and that of continuous currents many of the details related to their equator-crossing were shown by NB to be similar. Specifically, the simulation of both particles and continuous currents shows that the equator acts as a "splitter" in the sense that in both a fraction of the particles/current does not cross the equator into the other hemisphere and, instead, it recirculates and remains in its hemisphere of origin. A careful analysis of the dynamics associated with this "splitting" of meridionally moving particles/current at the equator is the second focus of the present study and both points are addressed in the context of particle dynamics.

The common thread that connects the two foci of the present paper is the transport of AABW into the Northern Hemisphere. The meridional cross-section of Whitehead and Worthington (1982) indicates that the AABW core (i.e., water with potential temperature less than about 1°C) is entirely missing north of the equator. The NB compilation of data quantifies this diminishing of the transport with latitude in the Atlantic Ocean and shows that the decrease

of this transport between 30°S and the equator is not uniform. From 7 Sv at the south end of the Brazil basin (30°S) the AABW transport decreases only slightly to 6.7 Sv at 23°S and to 5.5 Sv at 11°S – for a total decrease of 20% (1.5 Sv) in over 20 degrees of latitude. In contrast, upon reaching the vicinity of the equator the AABW transport decreases abruptly to about 2 Sv only – a decrease of 65% (3.5 Sv) in just a few degrees of latitude! The data of Whitehead and Worthington (1982) shows that the fast decrease in the AABW transport continues into the Northern Hemisphere and at 2°N it is only a fraction of 1 Sv. The scenario in the Pacific and Indian Oceans is not as well documented as in the Atlantic Ocean but the available scant observations indicate a qualitatively similar picture. This observation supports the theoretical conclusion reached by NB that the equator acts as a "splitter" of the AABW current as it does for a cloud of particles. The small decrease of AABW transport in the 20 degrees of latitudes south of 11°S can be attributed to mixing with the overlying water but the larger decrease near the equator is, presumably, caused by the additional "equatorial effect."

The two issues addressed in the present work are: (i) the changes in angular momentum that occur when water columns flow from Antarctica to the equator, and (ii) the dynamics of equator crossing along the ocean's bottom are both studied by transforming the Lagrangian momentum equations to an angular momentum form. This, in turns, allows the construction of a Hamiltonian function of the 2-degrees-of-freedom (2DOF) dynamical system and its two pairs of conjugate variables. The same transformation was employed in the study of cross-equatorial flow under prescribed, meridional, pressure gradient (Dvorkin and Paldor, 1999) and for quantifying the zonal drift of particles that move on the surface of the rotating earth with time-dependent velocity (Paldor, 2001).

This paper is organized as follows. In section 2 we develop the Hamiltonian form of the system that describes the motion of a deep-water eddy along the bottom of a parabolic meridional channel. The Hamiltonian formulation of the dynamics is applied to the equatorward

motion from Antarctica to the equator in section 3 by combining analytical results with numerical integrating the momentum equations in mid-latitudes. An application of the same formulation to describe the equator-crossing process, as well as the details of the "splitter" role of the equator is carried out in Section 4. The two regimes are combined in Sec. 5 to the entire trajectory of an AABW eddy from Antarctica to the equator and from the equator to either of the poles. The paper concludes in section VI with some closing remarks.

2. Hamiltonian formulation and analysis of the transport equations

We envision the geometry outlined in Fig. 1 in which a deep (cold water, e.g. AABW) eddy moves along the bottom of a parabolic channel whose axis is directed in the meridional direction (φ) and its depth varies in the longitudinal direction (λ). We regard the center of mass of the eddy as a particle that obeys the momentum equations:

$$U_t = V\sin(\varphi)\,[2\Omega + U/R\cos(\varphi)] - g' h_\lambda/R\cos(\varphi), \qquad (2.1a)$$

$$V_t = -U\sin(\varphi)\,[2\Omega + U/R\cos(\varphi)], \qquad (2.1b)$$

where U and V are the velocity components in the zonal (λ) and meridional (φ) directions, respectively, Ω and R are Earth's rotation rate and radius, respectively, g' is the reduced gravity ($g' = g(\rho_1 - \rho_2)/\rho_1$, with g the gravitation vector and ρ_1 and ρ_2 the densities of the water in the eddy and in the overlying water, respectively) and h is the height of the channel's bottom above its maximal value at the centerline. We assume that the channel's bottom is parabolic in λ i.e. $h(\lambda) = H(\lambda/\Delta\lambda)^2$ so that $h(\lambda)$ increases from zero at the centerline $\lambda = 0$ to H atú λê $\Delta\lambda$. In these equations both the variation of the Coriolis parameter, $2\Omega\sin(\varphi)$, with φ and the curvature of earth's surface (via the metric terms $U/[R\cos(\varphi)]$) are fully taken into account. Subscripts of variables indicate derivatives (e.g. λ in 2.1a) and time-derivative on the LHS is the Lagrangian

derivative. In the following, the numerical subscript “0” will indicate an initial value and the subscript “s” will indicate a special (e.g. steady) value or function. The momentum equations (2.1a,b) are an extension of the momentum equations in NB, which are valid on the equatorial β-plane, to the global scale.

In addition to these momentum equations, the eddy’s coordinates vary with time as:

$$\lambda_t = U/R\cos(\varphi), \tag{2.1c}$$

$$\varphi_t = V/R. \tag{2.1d}$$

As was done in Dvorkin and Paldor (1999) (see also Paldor and Killworth, 1988) the set (2.1) is nondimensionalized so as to minimize the number of parameters appearing in the equations. The length and time scales that appear in system (2.1) are R and $(2\Omega)^{-1}$, respectively, so these are the natural choices for the scales to be used in the nondimensionalization. Accordingly, the velocity scale is $(2\Omega R) \approx 930$ m/s i.e. a dimensional oceanic velocity of 10 cm/s corresponds to a nondimensional velocity of about 10^{-4}.

The nondimensional form of system (2.1) is:

$$U_t = V\sin(\varphi)\,[1 + U/\cos(\varphi)] - \alpha\lambda/\cos(\varphi), \tag{2.2a}$$

$$V_t = -U\sin(\varphi)\,[1 + U/\cos(\varphi)], \tag{2.2b}$$

$$\lambda_t = U\cos(\varphi), \tag{2.2c}$$

$$\varphi_t = V, \tag{2.2d}$$

where U, V and t are now dimensionless and $\alpha = 2g'H/(2\Omega R\Delta\lambda)^2$. For typical oceanic values of $g' = 0.5 \times 10^{-2}$ ms^{-2}, H = 2000 m and $\Delta\lambda = 0.5$ Radian, α is of order 10^{-4}. Note that the single parameter of system (2.2) - α - augments the 5 parameters (g', R, Ω, H, Δλ) of system (2.1).

Although system (2.2) conserves the total (kinetic + potential) energy it does not have a Hamiltonian function and in the next subsection we obtain a Hamiltonian form for system (2.2).

(a) *Canonical form of the dynamical system*

The way to write system (2.2) in a Hamiltonian form is to substitute the angular momentum for the zonal velocity. In nondimensional form, the angular momentum, D, is:

$$D = \cos(\varphi)(\cos(\varphi)/2 + U), \tag{2.3}$$

so that the zonal velocity can be recovered from the value of D via:

$$U = D/\cos(\varphi) - \cos(\varphi)/2. \tag{2.4}$$

When the total energy is written in terms of D instead of U the dynamical system is Hamiltonian and its Hamiltonian function given by:

$$H(V, \varphi, D, \lambda) = {}^1/_2(V^2 + (D/\cos(\varphi) - \cos(\varphi)/2)^2 + \alpha\lambda^2), \tag{2.5}$$

with (V, φ) and (D, λ) its two pairs of conjugate variables satisfying the canonical equations:

$$\varphi_t = V = H_V, \qquad V_t = {}^1/_2\sin(2\varphi)\,[{}^1/_4 - D^2/\cos^4(\varphi)] = -H_\varphi; \tag{2.6a}$$

$$\lambda_t = D/\cos^2(\varphi) - {}^1/_2 = -H_D, \qquad D_t = -\alpha\lambda = -H_\lambda\,. \tag{2.6b}$$

Set (2.6) is the sought canonical form of the eddy translation model. It can be easily verified that the Hamiltonian function in (2.5) remains constant with time. When the channel's bottom is flat ($h(\lambda)$=const.) or when gravity is set equal to zero $\alpha = 0$, D is conserved according to (2.6b), and the 2-degrees-of-freedom system (2.6) has 2 integrals of motion, H and D, so the system is integrable. This case, which was completely solved by Paldor and Sigalov (2001) is a natural starting point for analyzing system (2.6). We briefly summarize the findings of the "inertial" system that are relevant to the present study.

(b) *The inertial dynamics*

Setting $\alpha = 0$ in system (2.6) results in the inertial system that describes the free motion of a mass-point (e.g. an AABW eddy) on the rotating earth, which was studied thoroughly in Paldor (2001) and Paldor and Sigalov (2001). Equation (2.6b) implies that the, constant, D is a model parameter of the reduced, 1DOF, system (2.6a), which is obviously integrable. The cyclic

coordinate $\lambda(t)$ is determined by the constant value of D and $\varphi(t)$ according to $\lambda_t = D/\cos^2[\varphi(t)] - 1/2$.

The Hamiltonian in the inertial case is given by the kinetic energy (with U replaced by D):

$$H_{inertial}(V, \varphi; D) = 1/2\ (V^2 + [D/\cos(\varphi) - \cos(\varphi)/2)^2]. \qquad (2.7)$$

(Note: D is a variable in 2.5 but it appears as a parameter in 2.7 although $\lambda_t = \partial H_{inertial}/\partial D$!)

The findings of Paldor (2001) and Paldor and Sigalov (2001) are that for D > _ the (V, φ) dynamics has a single elliptic fixed point on the origin. At this equatorial ($V = 0 = \varphi$) fixed point the motion is directed eastward with constant speed $U=D-1/2 > 0$. Near this point the system oscillates in (V, φ) with frequency $(D^2-1/4)^{1/2}$. averaged (over (V,φ) oscillation) increase in longitude, $<\lambda(t)>$, is given by:

$$<\lambda(t)> = (D-1/2) + D\delta E/(D^2-1/4), \qquad (2.8)$$

where $\delta E = 1/2 V^2$ ê$_{\varphi=0}$ is the value of $H_{inertial}$ above its value of $1/2\ (D - 1/2)^2$ at the fixed point.

This averaged longitude increase has two contributions: The first, $D - 1/2 = U > 0$, is due to the eastward zonal velocity along the equator (see Eq. 2.4) and the second term is due to the drift assocaited with the averaged (over the period $T = 2\pi/(D^2 - 1/4)^{1/2}$) oscillatory motion, which is also directed wastward when $D > 1/2$.

The $D = 1/2$ case (i.e., U vanishes along the equator) is the, highly degenerate, bifurcation point where no elliptic fixed points exist anywhere and the dynamical analysis requires higher (than linear) order expansion near the equator. Numerical integration of the momentum equations, however, shows that the eastward drift occurs in this case and even for D slightly less than $1/2$ provided the energy is sufficiently high (see Paldor and Killworth 1988) but no simple formula is available for quantifying it (the expression involves elliptic integrals).

For $D < 1/2$ the equator becomes a hyperbolic fixed point (so the linearized motion near it, is exponential in time) and two elliptic fixed points occur at latitudes $\varphi_{ell} = \pm\arccos([2D]^{1/2})$. A linear analysis near the new elliptic points ($V_{ell} = 0$, $\varphi_{ell} = \pm\arccos([2D]^{1/2})$ shows that the

frequency of the oscillation in (V, φ) near these points equals $\sin(\varphi_{ell})$ (the Coriolis frequency) so the period of these, mid-latitude, inertial, oscillations is:

$$T = 2\pi/\sin(\varphi_{ell}) = 2\pi(1 - 2D)^{-1/2}. \qquad (2.9)$$

The zonal motion near these mid-latitude fixed points consists of oscillations with period (2.9) due to the oscillations in (V, φ) and westward directed drift at a rate given by:

$$\langle\lambda(t)\rangle = -\delta E/\sin^2(\varphi_{ell}) = -\delta E(1 - 2D)^{-1}. \qquad (2.10)$$

Here, δE is the value of $H_{inertial}$ above its value of 0.0 at ($V=0$, $\varphi = \varphi_{ell}$) and since the Hamiltonian is conserved, δE is determined only by the initial conditions of V_0, U_0 and φ_0 (or, alternatively, by V_0, φ_0 and the value of D).

A similar linear analysis near the hyperbolic, equatorial, fixed-point shows that system (2.6a) is unstable there so tiny small deviation from the fixed-point results in exponentially growing (with time) departure. Since $D < 1/2$ implies $U\hat{e}_{\varphi=0} < 0$ the conclusion is that the westward motion along the equator is unstable and trajectories are bound to be repelled from it.

To sum up the results of Paldor and Sigalov (2001): The intertial motion consists of 2 simple regimes: an equatorial regime where the eddy remains in one hemipshere and a mid-latitude regime where the eddy remains in one hemisphere, oscillating about a mean latitude (determined by D) while drifting westward.

(c) *Special solutions*

The new special solutions of system (2.6) listed here are designated by the subscript "s" and obtain by requiring that V_t vanishes identically. Steady solutions of system (2.6) are obtained by setting $\partial/\partial t = 0$ in all 4 equations and a straightforward calculation shows that these solutions satisfy:

$$V_s = 0 = \lambda_s; \qquad D_s(\varphi_s) = 1/2\cos^2(\varphi_s); \qquad \text{for any (constant) } \varphi_s. \qquad (2.11)$$

The steady solutions describe an eddy located at latitude φ_s on the channel's centerline with zero kinetic energy since both $U_s = 0$ (see Eq. 2.4) and $V_s = 0$ so the eddy remains in its location

at all times. Since $D_s = {}^1/_2\cos^2(\varphi_s) < {}^1/_2$ the analysis of Dvorkin and Paldor (1999) guarantees that all such steady states are elliptic in (V, φ) space (i.e. near (V_s, φ_s) V and φ can only oscillate with frequency sin(φ_s)) while (2.6b) insures that for fixed $\varphi = \varphi_s$ the linearized dynamics in (D, λ) is oscillatory too [with frequency $\alpha^{-}/\cos(\varphi_s)$].

The first, non-steady, special solution of (2.6) represents equatorial oscillations. It obtains by setting φ(t) = 0 in the V_t equation of (2.6a) so the eddy remains on the equator at all times, which mandates V = 0 as well. The dynamics in (D, λ), obtained by setting φ=0 in (2.6b), is oscillatory:

$$V_s=0; \quad \varphi_s(t)=0; \quad \partial D_s(t)/\partial t=\partial U_s(t)/\partial t=-\alpha\lambda_s(t); \quad \partial\lambda_s(t)/\partial t=(D_s(t) - {}^1/_2)=U_s(t). \quad (2.12)$$

This special solution describes harmonic oscillations of Ds, λ_s) on the equator (where the Coriolis force vanishes so no V_s is generated by the finite $U_s(t) = D_s(t) - {}^1/_2$). The Hamiltonian of this system is a "potential well," $H(U_s, \lambda_s) = {}^1/_2 (U_s^2 + \alpha\lambda_s^2) = {}^1/_2 [(D_s-{}^1/_2)^2 + \alpha\lambda_s^2]$ and the frequency of these equatorial oscillations is $\alpha^{1/2}$. The conservation of energy implies that the zonal speed in this equatorial potential well, ú$U_s(t)$ê, is determined by the absolute value of the "angle", ÷$\lambda_s(t)$ê, via ú$U_s(t)$ê= $(2E) - \alpha\lambda_s(t)^2)^{1/2}$, where E is the value of H (i.e. either ${}^1/_2 U_s^2$ê$_{\lambda=0}$ or ${}^1/_2\alpha\max[\lambda_s(t)^2]$) so $-(2E)^{1/2} \le U_s(t) \le (2E)^{1/2}$.

For 0 <÷V_sç << ÷U_sç in system (2.6) φ can no longer be set equal to zero at all times. However, one can naively deduce that the special solution, Eq. (2.12), describes the dynamics only to 1st order in φ bu we will shortly show that this solution is unstable so small deviations from it are repelled from the equator.

The second, non-steady, special solution of (2.6) approximates the mid-latitudes geostrophic motion. It obtains by setting $D_s = {}^1/_2\cos^2(\varphi_s)$ in the V_t equation in (2.6a) to ensure that V_t =0 so that V_s is constant, but different from zero. Since for oceanic speeds ÷V_sç=$O(10^{-4})$ is small, the terms proportional to V_s^2 can be considered second order. Since $D_s={}^1/_2\cos^2(\varphi_s)$, the value of λ_s via the D_t equation in (2.6b):

$$\lambda_s = -D_t/\alpha = (1/2\alpha)\sin(2\varphi_s)V_s. \qquad (2.13)$$

Note that differentiation of Eq. (2.13) with respect to time yields $\partial\lambda_s/\partial t = \cos(2\varphi_s)V_s^2/\alpha$, which is quadratic in V_s: positive (eastward) for $\varphi_s < 45°$ and negative (westward) for $\varphi_s > 45°$. It follows from (2.13) that $\sin(2\varphi_s)V_s = \alpha\lambda_s/\sin(2\varphi_s)$ which is simply the geostrophic balance between the zonal presure gradient at λ_s (see 2.2a) and the Coriolis force $\sin(\varphi_s)\, V_s$.

To sum up, to first order in V_s, the mid-latitude (geostrophic) special solution is:

$$V_s = 2\alpha\lambda_s/\sin(2\varphi_s); \quad \varphi_s(t) = \varphi_0 + V_s t; \quad D_s(\varphi_s) = {}^1/_2\cos^2(\varphi_s); \quad \lambda_s = \sin(2\varphi_s)V_s/(2\alpha), \qquad (2.14)$$

so $\varphi_s(t)$ and $D_s(t)$ are linear in V_s and $\lambda_s(t)$ and $V_s(t)$ – quadratically (but V_s is constant!).

This special solution is realized only for $V(0) = V_s$. It will be **approximately** realized for $V(0) = 0$ provideed $V_s << 1$ (see Fig. 2). However, if V_s is **not** small **or** $V(0) = 0$ this solution does not provide a reasonable approximation and an averaged trajectory is now derived for this case.

(d) Averaged (slow) trajectory

In addition to the two special solutions found above, an averaged trajectory can be constructed analytically where the fast oscillatory (orginating in the inertial motion part of the trajectory is filtered out and the slow monotonic motion is the sole contributor to the trajectory. A similar averaging out of fast oscillations was done by Paldor (2001) in the computation of the zonal drift associated with the inertial oscillations in mid-latitudes on the rotating earth.

In the present problem the averaged trajectory obtains by realizing that for fixed $D < {}^1/_2$ the (inertial) oscillaations in (V, φ) have, according to (2.6a), a frequency of $(1 - 2D)^{1/2} = \sin(\varphi_{ell})$. For fixed φ, on the other hand, the frequency of oscillation in (D, λ) is $\alpha^{1/2}/\cos(\varphi)$ (see 2.6b). Since in mid-latitudes, $\sin(\varphi_{ell}) \sim 0.5$ while $\alpha^{1/2}/\cos(\varphi) \sim 10^{-2}$ for realistic values in the ocean, we can safely assume that D is constant in the course of a single (V,φ) oscillation. Thus, when D is **fixed** the formula for the zonal drift (that filters out the (V,φ) oscillations from the inertial

trajectory) developed in Paldor (2001, Eq. 5.8) applies straightforwardly in the present case. Accordingly, the coordinates $D^{av}(t)$ and $\lambda^{av}(t)$ that correspond to the averaged trajectory satisfy:

$$\lambda^{av}(t)_t = -D/(1 - 2D^{av}) ; \qquad D^{av}(t)_t = -\alpha\lambda^{av} , \tag{2.15}$$

where $E = H - {}^1/_{2\alpha(\lambda^{av})^2}$. The latitude temporal changes are determined from $\cos^2[\varphi^{av}(t)] = 2D^{av}(t)$ and the calculation of V(t) is redundant. This averaged trajectory extends the 2nd special solution to the case when the initial velocity V(0) differs significantly from $V_s = 2\alpha\lambda(0)\sin[2\varphi(0)]$.

(e) *Stability of special solutions*

An important characteristic of any solution of a dynamical system is its stability, which determines the temporal evolution of small amplitude deviations (perturbations) from it. In order to assess the stability of a special solution one has to linearize system (2.6) near it and assume that the temporal evolution of the perturbations (to all 4 variables) is given by $e^{\mu t}$ where μ can be complex. When $Re\{\mu\}$ is real positive the perturbations grow exponentially in time so after some finite time the perturbations are no longer small.

Applying this procedure to system (2.6) one gets a quadratic equation for μ^2, which has to be negative for stability. The condition $U^2 < 0$ is guaranteed provided:

$$4D_s^2\tan(\varphi_s)^4 > \cos(2\varphi_s)[{}^1/_4 - D_s^2/\cos(\varphi_s)^4]. \tag{2.16}$$

This condition is always satisfied by the steady state and by the mid-latitude special solution (as well as by the average solution) for $\varphi_s \neq 0$ since in both cases $[{}^1/_4 - D_s^2/\cos(\varphi_s)^4]$ vanishes while the left-hand side (LHS) of Eq. (2.16) is positive. However, in the equatorial oscillation special solution, however, this condition is violated since for $\varphi_s = 0$ the LHS vanishes identically but the right-hand side (RHS) is positive for $D < {}^1/_2$. Thus, for westward motion, $U = D - {}^1/_2 < 0$, the equatorial special solution is unstable and the trajectory is repelled from the equator while for eastward motion, $U = D - {}^1/_2 = > 0$, the RHS of (2.16) is negative so that the solution is stable and the particle remains close to the equator.

These results are invoked in the next two sections to explain the two focal issues of this study.

3. Mid-latitude motion

The first issue addressed in this work is the dynamical description of the trajectory of a dense eddy from Antarctica to the Tropics and the angular momentum balance along this trajectory.

The geostrophic special solution given by Eq. (2.14) applies to mid-latitude motions off the channel's bottom. To first order, the velocity in this special solution is meridionally directed, $V = 2\alpha\lambda/\sin(2\varphi)$, and geostrophic: the Coriolis force, $V\sin(\varphi)$, balances $-\alpha\lambda/\cos(\varphi)$, the force due to the sloping channel. An angular momentum view of this motion is that D increases continuously by the applied zonal pressure gradient force, $D_t = -\alpha\lambda$, but since the total energy is not altered, this change in D is manifested only in the continuous change in $\cos(\varphi)$ and not in U.

In addition to the geostrophic meridional velocity, there exists a 2nd order contribution to the cross-channel, zonal, motion given by $\lambda_t = \cos(2\varphi)V^2/\alpha$, directed westward at latitudes higher than 45° and eastward at latitudes lower than 45°.

These results are now confirmed by comparing them to numerical computed solutions of (2.2).

Numerical confirmation

System (2.2) was integrated numerically using a 5th order Runge-Kutta scheme with a tolerance of 10^{-9} to verify the analytical considerations and the geographical trajectories' characteristics. In the mid-latitude case, Fig. 2 shows the trajectories obtained from the initial conditions: $U(0) = 0$ (i.e., $D(0) = {}^1/_2\cos^2[\varphi(0)]$, $\varphi(0) = 60°S$, $\lambda(0) = -10°$ $V(0) = 2\alpha\lambda(0)/\sin[2\varphi(0)]$ (solid curve) and $V(0) = 0$ (dotted curve). The former curve shows the special solution Eq. (2.14)

while the latter (dotted) curve of Fig. 2 clearly demonstrates the oscillatory (i.e., stable) behavior of the system **near** the special solution (2.14), i.e., when $V(0) \neq 2\alpha\lambda(0)/\sin[2\varphi(0)]$. Since U(0) = 0 in both cases, the initial condition V(0) = 0 in the oscillatory curve implies according to Eq. (2.5) that $H = {}^{1}/_{2}\alpha\lambda(0)^2$ is the potential energy. Thus, at short times the potential energy can only decrease, to enable the increase in the kinetic energy (so that their sum remains constant), i.e., the eddy must start its trajectory with positive U so that ${}^{1}/_{2}\alpha\lambda^2$ can decrease.

The kinetic energy that develops is divided between two components, the meridional geostrophic velocity of the special solution (2.14) and the oscillations near this velocity. The only way to observe just one of these two sources is to impose the geostrophic velocity as the initial velocity as in the solid curve of Fig. 2. The monotonic (solid) curve of Fig. 2 also demonstrates the analytical conclusions regarding the 2nd order westward/eastward drift at latitudes poleward/equatorward of 45° which are masked by the oscillations in the thin-solid curve.

In a similar way to the equatorward motion shown in Fig. 2, poleward motion is only possible along the channel's east flank where $\lambda > 0$, so D decreases ($D_t = -\alpha\lambda$), which enables the increase in latitude.

A numerical confirmation of the validity of the averaged trajectory of section 2(d) is shown in Fig. 3 for the case where $V(0)/V_s$, i.e., when the geostrophic solution (dotted curve) approximates the actual trajectory (spiraling solid curve) very poorly. The averaged trajectory (solid curve inside spiral) reproduces the average of the actual trajectory with impressive accuracy, which underscores the advantage of the angular momentum paradigm, Eq. (15), over geostrophy, Eq. (2.14).

4. Equatorial trajectories

As was shown above, the motion of the eddy along the equator is oscillatory with frequency $\alpha^{1/2}$. The motion during the eastward segment of the oscillation is stable so that the eddy encounters no problem reaching the eastern end of the trajectory. In contrast, the motion along the westward segment of the oscillation is unstable so during this segment an expulsion of the eddy from the equaatorial oscillation regime is expected to occur. These results are now confirmed numerically.

Numerical confirmation

The numerical computation of the oscillations near the equators shown in Fig. 3 clearly confirms the analytic conclusions reached above. Right on the equator, the eddy oscillates with an $\alpha^{1/2}$ frequency as is evident from the phase space plot in Fig. 4a (the corresponding (λ, φ) plot is a trivial straight line) where kinetic energy is continuously exchanged with potential energy (while the Hamiltonian's value remains, of course, constant at all time). When the trajectory originates slightly off the equator, (e.g., 0.001° latitude – a mere 100 meters!) on the channel's western flank the results shown in Fig. 4b demonstrate that the eddy successfully completes the eastward segment of the oscillation while remaining close to the equator. This is consistent with the analytic result regarding the stability of the special solution along its eastward segment. By comparison, in the return (westward) segment of the oscillation the trajectory is unstable ($D < {}^{1}/_{2}$) and in agreement with this instability, the eddy in Fig. 4b is totally repelled from the equator during the westward segment of its second oscillation and never completes the oscillation. Similar behavior was also encountered in the numerical simulations on the equatori β-plane carried out by NB and Borisov and Nof (1998).

5. The combined trajectory: Relevance to observations

The presence of the AABW throughout the Western South Atlantic is well documented. The motion of this dense water can easilty be explained based on a force balance between the eastward directed pressure gradient force on the channel's western flank and the westward directed Coriolis force associated with an equatorward flow in the Southern Hemisphere. An alternative, angular momentum paradigm of the same motion follows from the equation $D_t = -\alpha\lambda$, which suggests that the only way for D to increase ($D_t > 0$) is for the eddy to move along the western flank of the channel where $\lambda < 0$. The continuous increase in D at fixed λ, when U^2 is not free grow beyond a maximal value set by the energy conservation, is accomplished by increasing $\cos(\varphi)$ (i.e., decreasing φ).

By the time an AABW eddy is located sufficiently close to the equator along the western flank, its angular momentum D has reached a value close to $^1/_2$ and the eddy is subject to the equatorial dynamics. Once in the equatorial oscillation control, the eddy moves eastward from its location on the western flank, crossing the channel's centerline and continuing to the eastern flank. During this segment of the oscillation the speed, proportional to $\alpha^{1/2}$, is much larger than in the mid-latitude motion so the eddy is expected to undergo efficient mixing with the surrounding water (i.e. dissipate faster).

Once the AABW eddy has reached the maximal longitude on the channel's eastern flank (where U = 0) near (but not at) $\varphi = 0$ its D value has decreased to a value at or below $^1/_2$. Upon commencing its westward segment of the equatorial oscillation the D value is further decreased ($U < 0$) so that the motion becomes unstable. On the westward unstable segment the eddy can either be expelled from the equator (to mid-latitude motion in one of the two hemispheres) or complete its equatorial oscillation and return to the western flank while increasing the (φ, V) values relative to their values on the eastward segment. As was shown in Fig. 4, both scenarios are encountered in dissipation-free simulations of system (2.2) with equal probabilities. Since the

expulsion of the eddy from the equator takes place only on the westward segment only it is clear why no AABW water can be found in the Western North Atlantic.

The process of dissipation (mixing) of the eddy's dense water was completely ignored up to this point but it can be easily linked either to the shear associated with the eddy's motion in the quiescent overlying ocean water or to bottom friction. Thus, in the context of system (2.2), regardless of its origin, mixing can be simply modeled by adding a dissipation term, proportional to the eddy's velocity, to the momentum equations (2.2a,b). Accordingly, the steady state in which the eddy does not at all move is considered as a state of complete mixing. For small enough dissipation terms and finite times the structure of the dissipative system differs only slightly from that described above and the trajectory will slowly spiral to the steady state along the channel's centerline.

For reasons that are beyond the scope of this work (the inherent eastward equatorial drift, see Paldor, 2001) the addition of dissipation makes the westward segment of the equatorial oscillation even more difficult to complete. This increases the likelihood of the eddy leaving the equator, thus commencing the mid-latitude, geostrophic, poleward directed motion early in its westward segment. An example of the combined trajectory when dissipation (with a dissipation coefficient of 0.001) is included in (2.2) is shown in Fig. 5. The tendency of the eddy to leave the equator early during the westward segment of the oscillation, i.e. while it is located on the western flank, is clear in the geographic trajectory (Fig. 5a). Dissipation of energy is dramatic both during (the eastward segment of) the equatorial oscillation and **near** the mid-latitude motion whereas in the mid-latitude, geostrophic, motion energy loss is negligible due to the slow velocities involved. This correlation between changes in energy and longitude is clearly evident in Fig. 5b.

The sensitive transition from mid-latitude, geostrophic flow to the equatorial oscillation regime is the cause of the "splitter" effect encountered in the numerical simulation of NB on the

equatorial β–plane. The equatorial dynamics is, in fact, a barrier to meridional motion along the channel's western flank while along its eastern flank it allows some of the eddies to move meridionally while other eddies return westward. This is compounded by the fast dissipation in the equatorial oscillations so that by the time the eddy leaves the equator and commences its poleward motion, it has dissipated a large fraction of its water to the surrounding ocean water.

6. Summary

The main findings of this work can be summarized as follows:

1. The trajectory of AABW eddies into the Northern Hemisphere is described by a 2DOF system that has only one integral of motion, implying the existence of chaotic bands.

2. The entire trajectory is made up of two parts, in each of which the motion is simple. In mid-latitudes is nearly steady, geostrophic, meridionally directed, along a fixed longitude. On the equator the motion is oscillatory as in a parabolic channel with no rotation.

3. The, slow, geostrophic motion in mid-latitudes occurs on the channel's western flank and is compounded by a 2^{nd} order zonal motion, which is westward-directed (up-channel) poleward of 45° and eastward-directed equatorward of it.

4. On the equator, the oscillation occurs at a large speed so that the eddy is dissipated efficiently. The oscillation's eastward segment is stable so the dissipated eddy reaches the channel's eastern flank but along its return segment the eddy is expelled from the equator due to the inherent instability of the westward motion. Dissipation reduces the likelihood of the eddy returning to the western flank on the westward segment of the equatorial oscillation. The dissipated eddy moves poleward along the channel's eastern flank in either hemisphere with equal probability.

Acknowledgement

This study was supported by a research grant from the US-Israel Binational Science Foundation to the Hebrew University and to the Florida State University.

Figure Captions

Fig. 1. The geometry of the meridional, parabolic, channel on the spherical earth. The spherical earth itself is missing from the figure and only the channel is portrayed. The longitude scale is arbitrary (bottom shoaling depends on $\Delta\lambda$) and the vertical axis is the height from the earth's center i.e. the ratio of channel's depth to earth's radius is greatly exaggerated.

Fig. 2. The geostrophic, mid-latitude, approximation (2.14) (solid curve) of the exact solution (dotted curve) (2.6). Note that a solution starting near the geostrophic special solution remains close to it at all subsequent times. The initial conditions are $\varphi(0) = 60°S$; $\lambda(0) = -10°$; $U(0) = 0$. $V(0) = 0$ for the actual solution (dotted curve) and $V(0) = 2\alpha\lambda(0)/\sin[\varphi(0)]$ (= geostrophic velocity) for the geostrophic solution (solid curve), final time is 210 and $\alpha = 0.01$. Similar results are obtained for other values of α or initial conditions. Note the westward (eastward) 2nd order drift poleward (equatorward) of the 45ˆlatitude.

Fig. 3.The slow, averaged trajectory in mid-latitudes (solid curve inside spiral), the actual trajectory (solid, spiraling curve) and the geostrophic special solution (dotted curve) for $\alpha = 0.001$. The averaged trajectory accurately filters out the (inertial) oscillations from the actual trajectory. The geostrophic solution provides a very poor estimate of the actual trajectory (and even reaches the South Pole) since $V(0) = -0.04$ whereas the initial northward velocity of the geostrophic special solution is $V_s = -0.002$ $(= 2\alpha\lambda(0)/\sin(2\varphi(0)])$. The other initial conditions are: $\lambda(0) = 50^{\circ}E$; $\varphi(0) = 30^{\circ}S$ and $U(0) = 0$ (i.e., $D(0) = 0.125$ for the averaged trajectory).

Fig. 4. *Equatorial Oscillations*. (a) Right on the equator: $\varphi(0) = 0$ (this oscillation is a straight line in (λ, φ) coordinates and is therefore depicted in $(\lambda, U=D-^{1}/_{2})$ phase space); and (b) Near the equator: $\varphi(0) = 0.001$ degree (i.e. 100 meters!). The other initial conditions are: $\lambda(0) = -10°$; $V(0) = 0 = U(0)$ and the value of α is 0.001. The instability of the equatorial

is evident in the growing distance between the curve in (b), which takes place only during the unstable westward segment but not during the stable eastward segment.

Fig. 5. The combined trajectory including the Antarctica-to-equator, equatorial oscillation and equator-to-pole regimes. A small dissipation term [-0.001*(U,V)] is added to the momentum equations (2.2a,b) to account for the mixing of the dense water eddy and the surrounding water. (a) Geographic trajectory. (b) Energy (dotted curve, left abscissa) and longitude (solid curve, right abscissa) versus time. Dissipation occurs mostly in segments of the trajectory with large longitudinal excursions (where the velocity is large).

References

Borisov, S. and D. Nof (1998). Deep, cross-equatorial eddies. *Geophys. Astrophys. Fl. Dyn.,* **87,** 273–310.

Dvorkin, Y. and N. Paldor (1999). Analytical considerations of Lagrangian Cross–Equatorial flow. *J. Atmos. Sci.,* **56(9),** 1229–1237.

Nof, D. and S. Borisov (1998). Inter-hemispheric oceanic exchange. *Q. J. R. Meteorol. Soc.,* **124,** 2829– 2866.

Paldor, N. (2001). The zonal drift associated with time-dependent particle motion on the earth. *Q. J. Roy. Meteor. Soc.,* **127(577A),** 2435–2450.

Paldor, N. and P. D. Killworth (1988). Inertial Trajectories on the Rotating Earth. *J. Atmos. Sci.,* **45,** 4013–4019.

Paldor N. and A. Sigalov (2001). The mechanics of inertial motion on the earth and on a rotating sphere. *Physica D,* **160(1-2),** 29–53.

Stommel, H. (1958). The abyssal circulation. *Deep-Sea Res.,* **5,** 80–82.

Stommel, H and A. B. Arons (1960a). On the abyssal cisrculation of the world ocean: I. Stationary planetary flow patterns on a sphere. *Deep-Sea Res.,* **6,** 140–154.

Stommel, H and A. B. Arons (1960b). On the abyssal circulation of the world ocean: II. An idealized model of the circulation pattern and amplitude in oceanic basins. *Deep-Sea Res.,* **6,** 217–233.

Whitehead, J. A. and L. V. Worthington (1982). The Flux and Mixing Rates of Antarctic Bottom Water Within the North Atlantic. *J Geophys. Res.,* **87(C10),** 7903–7924.

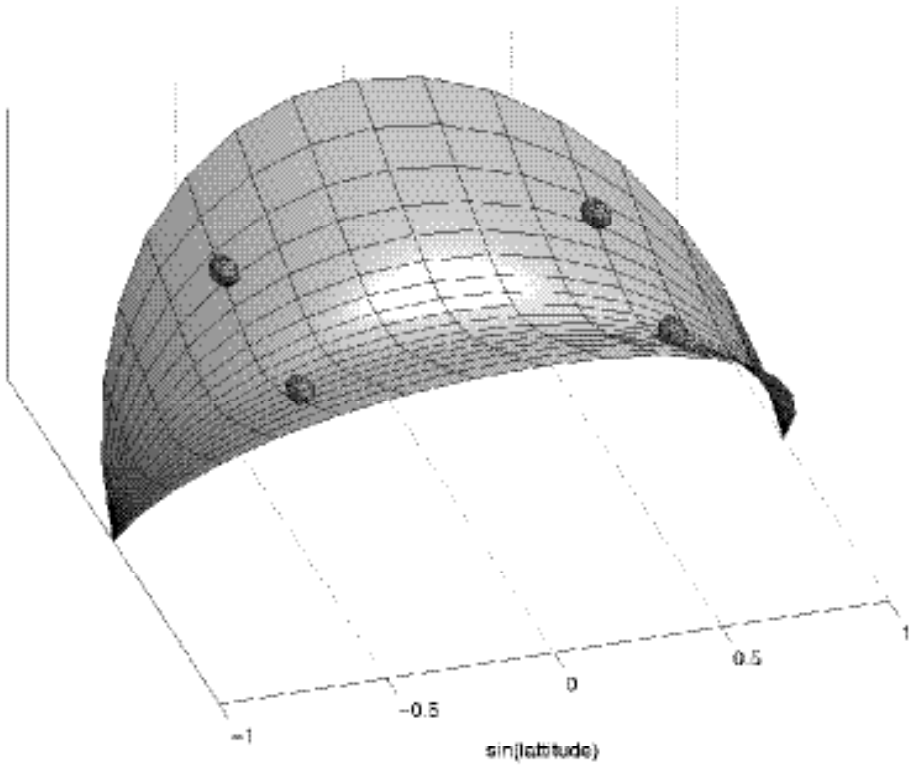

Fig. 1. The geometry of the meridional, parabolic, channel on the spherical earth. The spherical earth itself is missing from the figure and only the channel is portrayed. The longitude scale is arbitrary (bottom shoaling depends on $\Delta\lambda$) and the vertical axis is the height from the earth's center i.e. the ratio of channel's depth to earth's radius is greatly exaggerated.

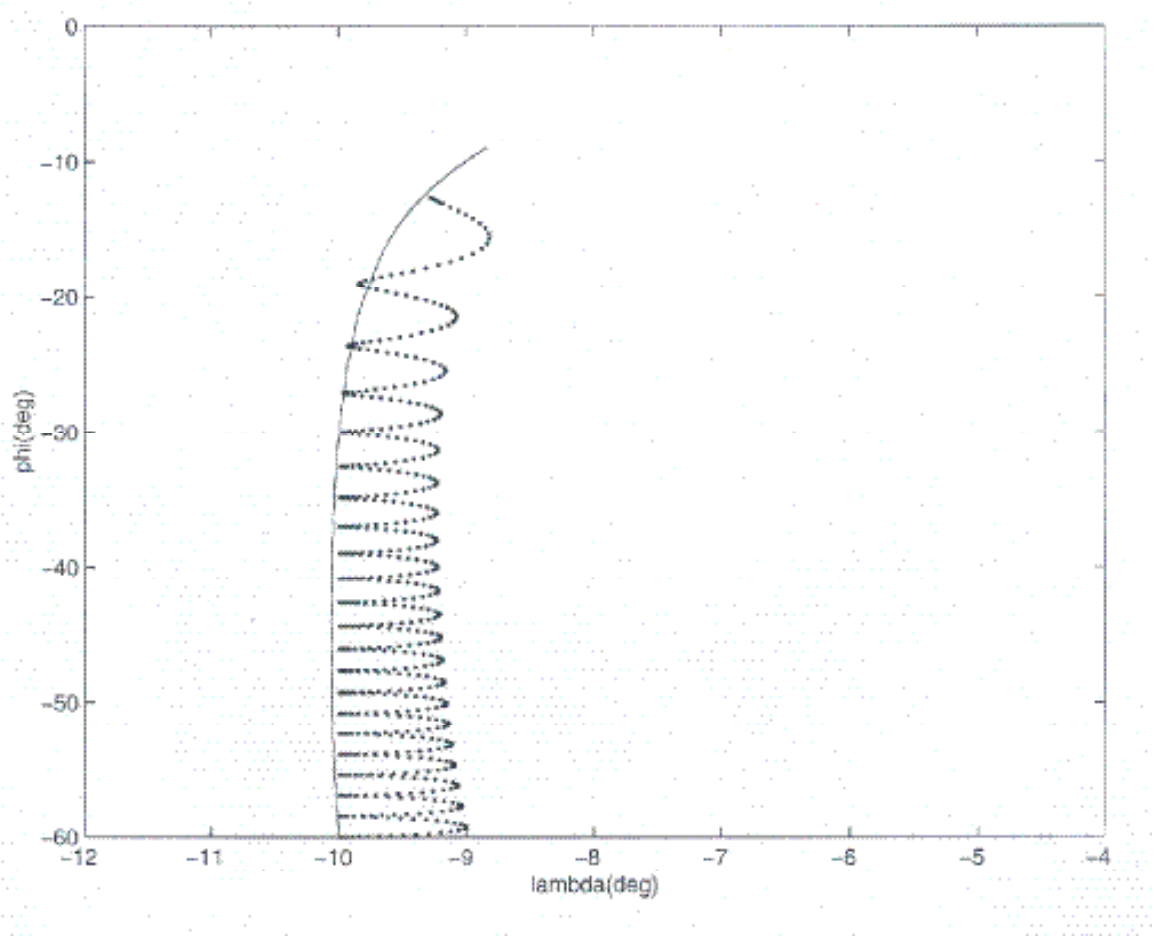

Fig. 2. The geostrophic, mid-latitude, approximation (2.14) (solid curve) of the exact solution (dotted curve) (2.6). Note that a solution starting near the geostrophic special solution remains close to it at all subsequent times. The initial conditions are φ(0) = 60°S; λ(0) = -10° ; U(0) = 0. V(0) = 0 for the actual solution (dotted curve) and V(0) = 2αλ(0)/sin[φ(0)] (= geostrophic velocity) for the geostrophic solution (solid curve), final time is 210 and α = 0.01. Similar results are obtained for other values of α or initial conditions. Note the westward (eastward) 2nd order drift poleward (equatorward) of the 45ˆlatitude.

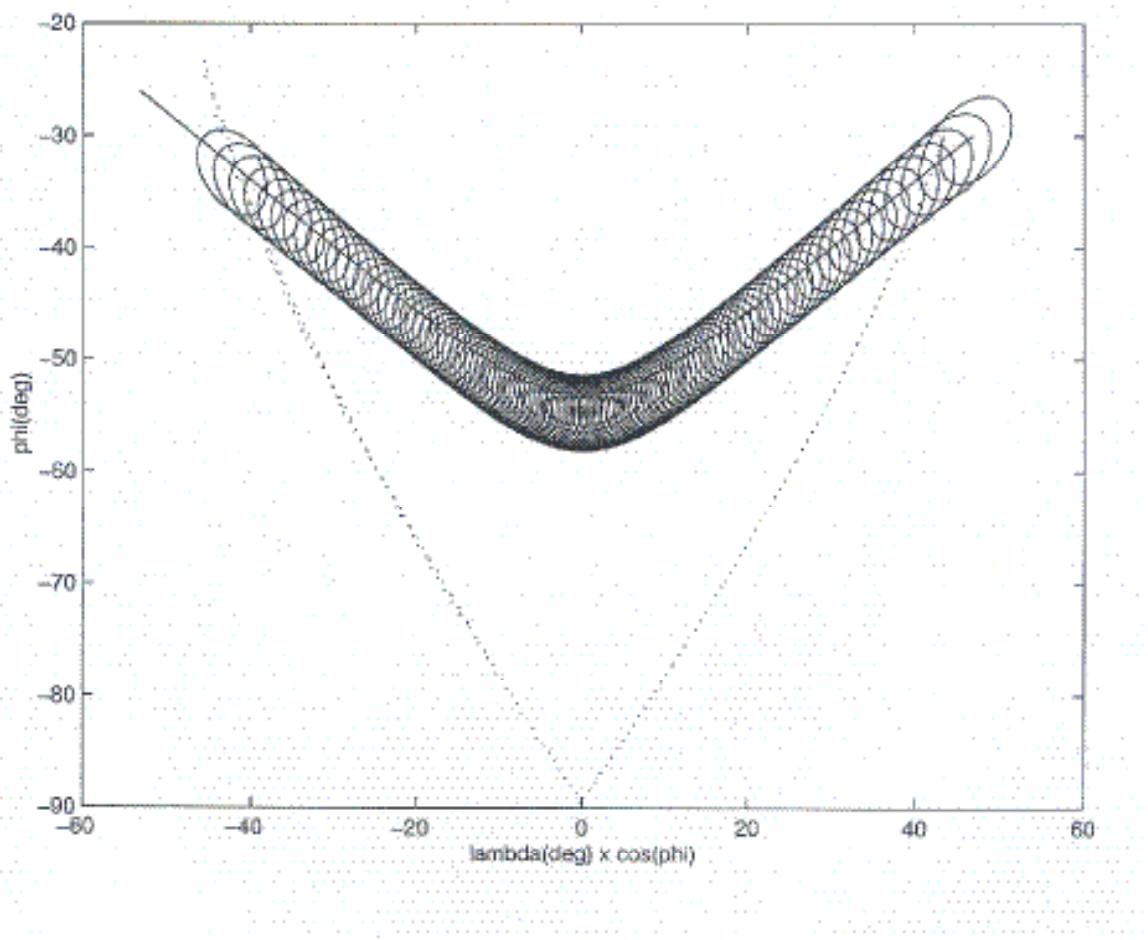

Fig. 3. The slow, averaged trajectory in mid-latitudes (solid curve inside spiral), the actual trajectory (solid, spiraling curve) and the geostrophic special solution (dotted curve) for $\alpha = 0.001$. The averaged trajectory accurately filters out the (inertial) oscillations from the actual trajectory. The geostrophic solution provides a very poor estimate of the actual trajectory (and even reaches the South Pole) since $V(0) = -0.04$ whereas the initial northward velocity of the geostrophic special solution is $V_s = -0.002$ $(= 2\alpha\lambda(0)/\sin(2\varphi(0))]$. The other initial conditions are: $\lambda(0) = 50^\circ$E; $\varphi(0) = 30^\circ$S and $U(0) = 0$ (i.e., $D(0) = 0.125$ for the averaged trajectory).

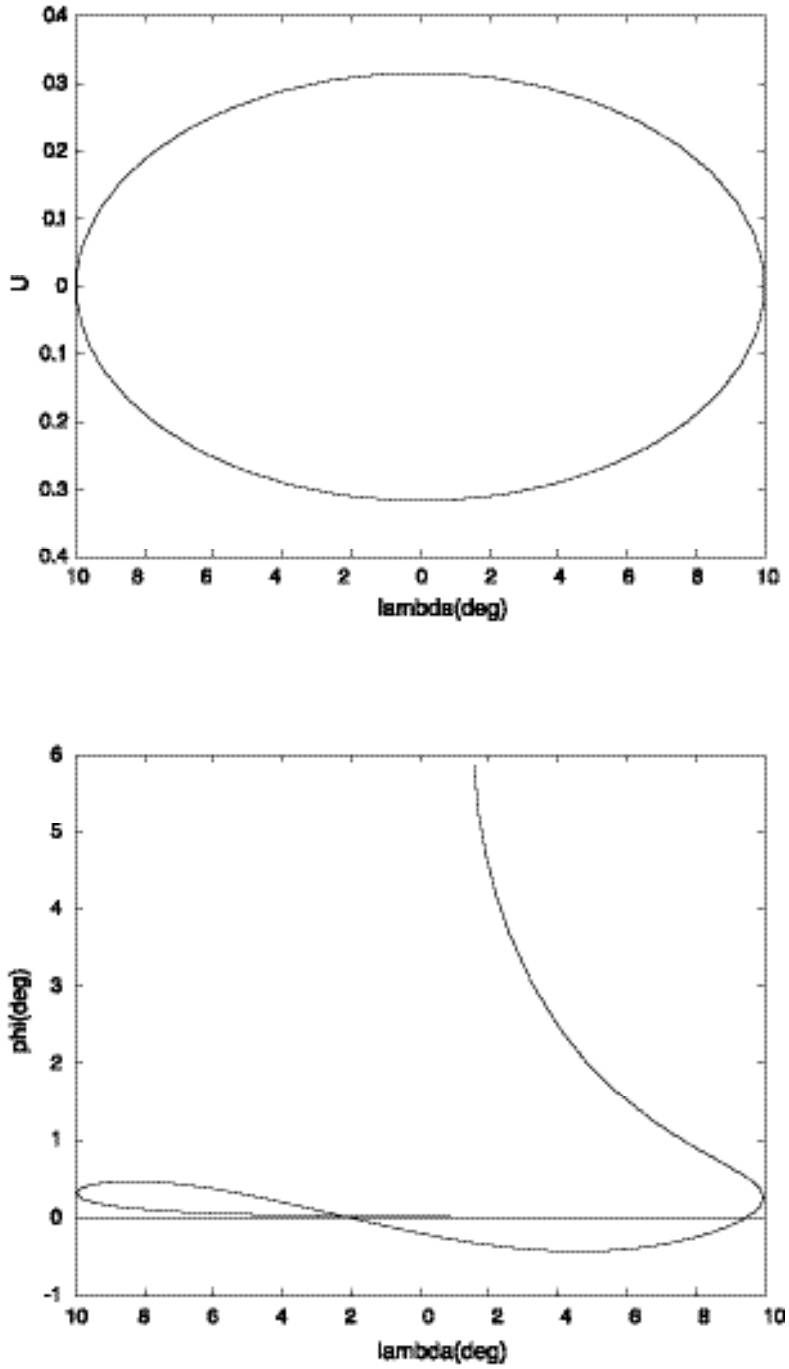

Fig. 4. *Equatorial Oscillations*. (a) Right on the equator: $\varphi(0) = 0$ (this oscillation is a straight line in (λ, φ) coordinates and is therefore depicted in $(\lambda, U=D-^{1}/_{2})$ phase space); and (b) Near the equator: $\varphi(0) = 0.001$ degree (i.e. 100 meters!). The other initial conditions are: $\lambda(0) = -10°$; $V(0) = 0 = U(0)$ and the value of α is 0.001. The instability of the equatorial is evident in the growing distance between the curve in (b), which takes place only during the unstable westward segment but not during the stable eastward segment.

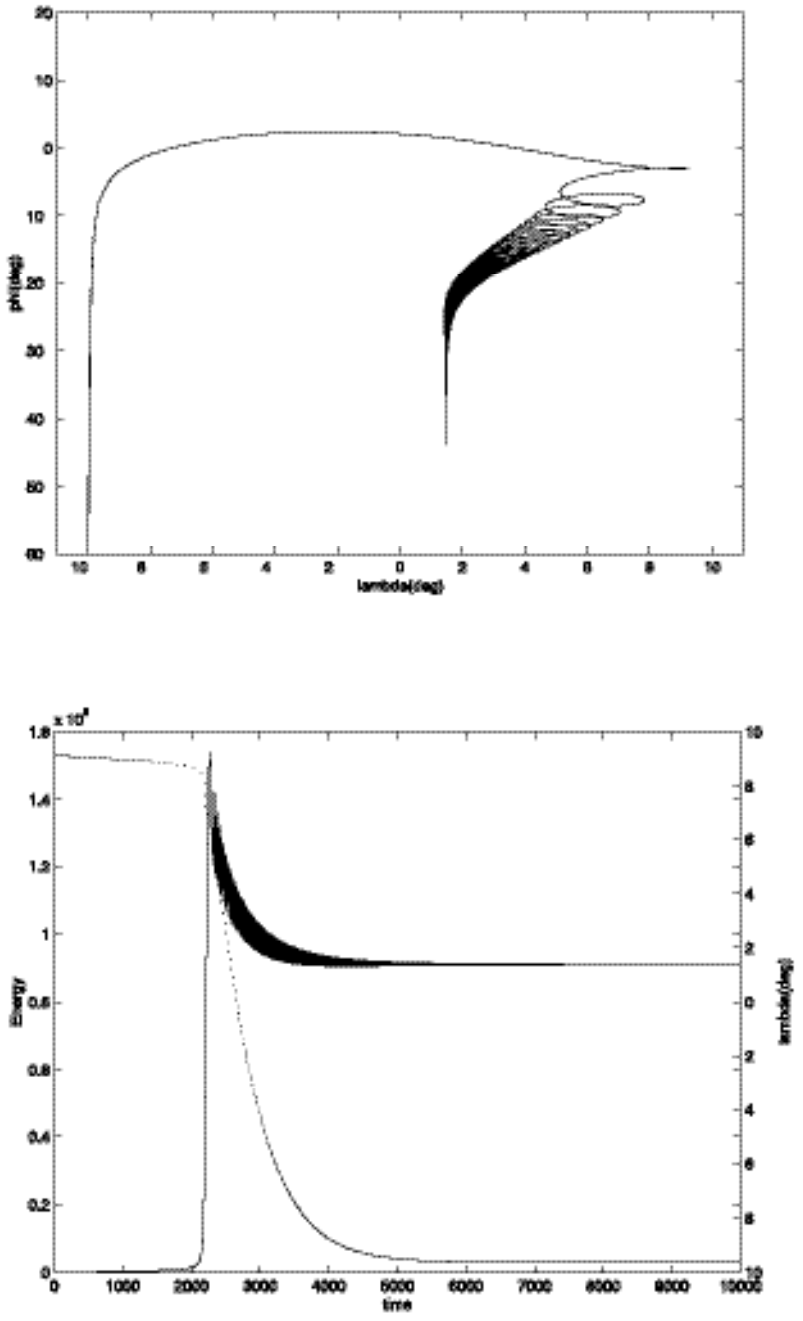

Fig. 5. The combined trajectory including the Antarctica-to-equator, equatorial oscillation and equator-to-pole regimes. A small dissipation term [-0.001*(U,V)] is added to the momentum equations (2.2a,b) to account for the mixing of the dense water eddy and the surrounding water. (a) Geographic trajectory. (b) Energy (dotted curve, left abscissa) and longitude (solid curve, right abscissa) versus time. Dissipation occurs mostly in segments of the trajectory with large longitudinal excursions (where the velocity is large).